Biosensors and Bioelectronics 126 (2019) 572–580

Contents lists available at ScienceDirect

Biosensors and Bioelectronics

journal homepage: www.elsevier.com/locate/bios

Electrochemical immunosensor utilizing electrodeposited Au nanocrystals and dielectrophoretically trapped PS/Ag/ab-HSA nanoprobes for detection of microalbuminuria at point of care

Muhammad Omar Shaikh[a], Pei-Yu Zhu[b], Cheng-Chien Wang[c], Yi-Chun Du[d], Cheng-Hsin Chuang[a,*]

[a] Institute of Medical Science and Technology, National Sun Yat-sen University, Taiwan
[b] Department of Mechanical Engineering, Southern Taiwan University of Science and Technology, Taiwan
[c] Department of Chemistry and Material Engineering, Southern Taiwan University of Science and Technology, Taiwan
[d] Department of Electrical Engineering, Southern Taiwan University of Science and Technology, Taiwan

ARTICLE INFO

Keywords:
Electrochemical immunosensor
Microalbuminuria
Interdigitated Microelectrodes
Nanoprobes
Dielectrophoresis

ABSTRACT

In this study, we have fabricated a simple disposable electrochemical immunosensor for the point of care testing of microalbuminuria, a well-known clinical biomarker for the onset of chronic kidney disease. The immunosensor is fabricated by screen-printing carbon interdigitated microelectrodes on a flexible plastic substrate and utilizes electrochemical impedance spectroscopy to enable direct and label free immunosensing by analyzing interfacial changes on the electrode surface. To improve conductivity and biocompatibility of the screen-printed electrodes, we have modified it with gold nanoparticles, which are electrodeposited using linear sweep voltammetry. To enable efficient immobilization of HSA antibodies, we have developed novel PS/Ag/ab-HSA nanoprobes (polystyrene nanoparticle core with silver nanoshells covalently conjugated to HSA antibodies), and these nanoprobes are trapped on the electrode surface using dielectrophoresis. Each immunosensor has two sensing sites corresponding to test and control to improve specificity by performing differential analysis. Immunosensing results show that the normalized impedance response is linearly dependent on albumin concentration in the clinically relevant range with good repeatability. We have also developed a portable impedance readout module that can analyze the data obtained from the immunosensor and transmit it wirelessly for cloud computing. Consequently, the developed immunosensing platform can be extended to the detection of a range of immunoreactions and shows promise for point of diagnosis and public healthcare monitoring.

1. Introduction

Microalbuminuria is the excretion of albumin in urine (30–300 mg/day or 30–300 mg/l in a morning urine sample) and is an important biomarker for the detection of Chronic Kidney Disease (CKD) (Forman et al., 2008; Glassock, 2010). Albumin, a water-soluble globular protein that comprises about one half of the total blood serum protein, is retained in the bloodstream when the kidneys are healthy. Persistent microalbuminuria is an indication that albumin is leaking through the vascular membranes of the kidneys and is an early sign of kidney damage as well as being an independent risk factor for incidence and fatality rate of cardiovascular disease (Jefferson et al., 2008). Regular screening of microalbuminuria, especially for higher risk patients such as those suffering from diabetes or hypertension, could enable early detection and effective treatment of CKD before it progresses to an irreversible stage. Some currently used technologies in hospitals and clinical laboratories include fluorescence immunoassays, high performance liquid chromatography, immunonephelometry and radioimmunoassay among others (Magliano et al., 2007; Lakowicz et al., 2005; Comper and Osicka, 2005). However, most of these technologies require well-equipped labs with sophisticated equipment, trained personnel to perform diagnosis, and are often time consuming. Thus, there is an urgent need for point of care (POC) immunosensing platforms that can quantitatively detect microalbuminuria in the clinically relevant range. In general, there has been a push for a range of POC technologies, which can perform the test anywhere from the home to the bedside, as they are more suitable for regular screening of diseases and public health monitoring (Gauglitz, 2014; da Silva et al., 2017; Dincer

* Corresponding author.
E-mail address: chchuang@imst.nsysu.edu.tw (C.-H. Chuang).

https://doi.org/10.1016/j.bios.2018.11.035
Received 16 September 2018; Received in revised form 11 November 2018; Accepted 20 November 2018
Available online 22 November 2018
0956-5663/

et al., 2017; Guo, 2018, 2017; Xu et al., 2018; Guo and Ma, 2017; Guo et al., 2018, 2015; Fu and Guo, 2018, 2017).

Only a few studies have been reported on the development of low cost quantitative POC platforms for detection of microalbuminuria and we have compared them in Table S1. Omidfar et. al. developed a sensitive and specific competitive immunosensor utilizing gold nanoparticle conjugated antibodies and PVA modified screen printed carbon electrode for detecting urinary albumin in the range of 20–200 μg/ml (Omidfar et al., 2011). Recently, Tsai et. al. developed an electrochemical immunosensor using screen printed electrodes and efficient direct covalent conjugation of antibodies to the electrode surface and can detect albumin in the relevant range (10–300 μg/ml) with a detection limit of 9.7 μg/ml (Tsai et al., 2016). However, further research in this area is needed to enable successful commercialization of immunological platforms that are suitable for POC detection of microalbuminuria. Currently, commercialized technologies for POC detection include conventional semi-qualitative urine dipsticks and quantitative testing using devices such as Hemoclue's Albumin 201 and Siemens's DCA-Vantage Analyzer. While the devices for quantitative detection are based on immunological methods with high per test cost, the accuracy of the calorimetric pH dependent dipsticks is questionable for the early detection of microalbuminuria.

Immunosensors, which detect the specific immune reaction of an antibody to its target antigen to form a stable complex, have seen significant growth in recent years for a range of applications from clinical diagnosis to environmental monitoring (Ricci et al., 2007; Wu et al., 2007; Saber et al., 2002). Label-free immunosensors, where the immune reaction can be directly monitored without the need for additional labelling and amplification steps are particularly suited for POC testing due to their speed and simplicity in operation. Labels such nanoparticles, fluorescent tags, quantum dots and enzymes can be used to improve sensitivity and selectivity of analyte detection for a range of immunosensors. However, there are issues associated with labels, which include additional costs, inherent multistep nature of analyses and potentially perturbative and non-specific signals. This has led to an increased interest in techniques that require no labelling and are inherently more facile and suitable for POC diagnostics (Chuang and Shaikh, 2017). Among the various transduction schemes utilized, electrochemical immunosensors have drawn much interest due to advantages like low cost, simplicity, reasonable limit of detection, ease of automation and integration with miniaturized readout and overall suitability for onsite testing (Ronkainen et al., 2010). Electrochemical immunosensors have been utilized for the detection of various analytical targets ranging from small molecules (e.g. haptens) and macromolecules (e.g. antigen and antibodies) to viruses and bacteria (Wen et al., 2016). Among the various interrogation techniques utilized in electrochemical immunosensors, Electrochemical Impedance Spectroscopy (EIS) is an effective technique for sensitive and label free monitoring of immunoreactions. Impedance based biosensors utilize the formation of a recognition complex between the antibody and its corresponding specific antigen in a thin film configuration on the electrode surface. This complex formation alters the capacitance and charge transfer resistance at the electrode/electrolyte interface. Since EIS uses small amplitude AC perturbation as opposed to DC based techniques like voltammetry, it can sensitively monitor changes in both the capacitance and electron-transfer resistance at this interface. Consequently, EIS has been used for direct sensing of affinity interactions like antigen-antibody, oligonucleotide-DNA and biotin-avidin as it helps bypass the labelling procedure normally needed for other electrochemical biosensors (Kharitonov et al., 2000; Athey et al., 1995; Bardea et al., 1999). Furthermore, integration of EIS with interdigitated electrodes has shown great promise in label free detection of biomolecules due to their ability to sensitively monitor electrical changes close to their surface (Yang et al., 2004; Chuang et al., 2016).

In this study, we have developed a simple disposable immunosensor for the detection of microalbuminuria using electrochemical impedance spectroscopy (EIS). The carbon interdigitated microelectrodes (IMEs) are fabricated using a one-step screen-printing protocol on flexible Polyethylene terephthalate (PET) substrates. Screen-printed electrodes not only address the issue of scalability and cost-effectiveness but also allow for portability, which is key for decentralized analysis (Taleat et al., 2014). Each immunosensor has two sensing sites corresponding to test and control to reduce the effects of non-specific absorption and increase specificity by performing differential analysis. To improve conductivity and biocompatibility, we have modified the surface of the carbon IMEs with gold nanocrystals that are obtained via electrodeposition. Electrodeposition is a simple and efficient technique that enables the gold nanocrystals to be evenly dispersed and firmly fixed on the surface of the electrode (Hezard et al., 2012). Recently, research on nanomaterials including noble metal nanoparticles, carbon nanomaterials and hybrid nanostructures has led to significant improvements in sensitivity and selectivity of a variety of electrochemical immunosensors (Abdorahim et al., 2016; Ju, 2011; Lim and Ahmed, 2016).

To improve antibody immobilization, we have synthesized novel nanoprobes (antibody conjugated nanoparticles) followed by trapping the nanoprobes on the surface of the IMEs using dielectrophoresis (DEP). These PS/Ag/ab-HSA nanoprobes consist of a polystyrene core with silver nanoshells (PS/Ag) to which the HSA antibodies (ab-HSA) are conjugated via covalent chemistry using a heterobifunctional Polyethylene glycol (PEG) ligand. We have developed an electroless plating protocol that can tune the size and density of the Ag nanoshells on the PS supporting core. These Ag nanoshells have significantly enhanced surface areas and can increase the number of immobilized antibodies and further improve charge transfer to and from the electrode surface. To improve physical immobilization of the nanoprobes on the IMEs, we have utilized DEP, which is an AC electrokinetic technique that can cause the translational motion of a dielectric particle in a suspended medium under the influence of an AC electric field (Pethig, 2017). In our previous work, we have utilized programmable DEP manipulation to distinguish bladder cancer staging using multiple antibodies on a single lab on a chip device (Chuang et al., 2015). The proposed immunosensing platform can detect HSA in spiked buffer solution with good repeatability and the normalized impedance response shows a linear dependence on HSA concentration in the clinically relevant range of 30–300 μg/ml. A schematic of the steps involved in immunosensor fabrication and operation is illustrated in Fig. 1. Furthermore, we have also developed a low cost and portable impedance readout module to which the immunosensor can be attached and results can be obtained at the point of care. The data can then be transferred wirelessly to a smart phone or computer and uploaded to the cloud database, thus enabling early detection and improved monitoring of CKD.

2. Experimental methods

2.1. Nanoprobe synthesis

The PS/Ag/ab-HSA nanoprobes consist of PS nanoparticles coated with Ag nanoshells conjugated to HSA antibodies. The conjugation of antibodies with nanoparticles has been widely utilized for developing immunosensors as it combines the novel intrinsic properties of nanoparticles and their enhanced surface areas with the selective and specific recognition capabilities of antibodies to antigens (Cardoso et al., 2012). While the dielectric PS NP core enables effective manipulation using DEP, the silver nanoshells provides a conductive channel to the electrodes and allow for oriented conjugation of antibodies via covalent chemistry.

2.1.1. PS nanoparticles via dispersion polymerization

The synthesis of water-soluble monodisperse PS nanoparticles consists of first preparing a chelating vinyl monomer, Glycidyl

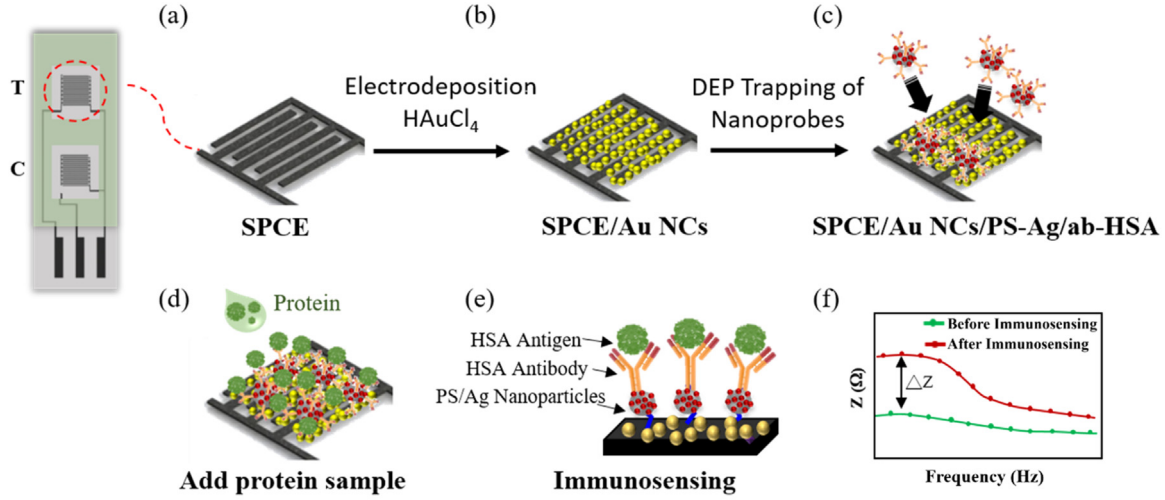

Fig. 1. Schematic illustration of systematic protocol for immunosensor fabrication and operation.

Methacrylate-Iminodiacetic Acid (GMA-IDA) followed by copolymerizing this monomer with styrene via dispersion polymerization. To obtain the GMA-IDA monomer, first IDA and ammonium hydroxide in a molar ratio of 1:2, respectively, are added to de-ionized (DI) water for acid-base neutralization and the solution is stirred until clear. Next, GMA (GMA: IDA molar ratio of 1:1) is added and the solution is heated at 65 °C for 2 h, resulting in the formation of GMA-IDA monomer, which is allowed to cool back to room temperature. Then we proceed to the synthesis of monodisperse polystyrene nanoparticles using dispersion polymerization. Briefly, styrene, GMA-IDA monomer, ethanol and water were added to a four-necked round bottom flask that is equipped with a thermometer, mechanical stirrer, N_2 gas inlet, condenser and heating mantle. The solution was first deoxygenated by bubbling with N_2 gas for one hour followed by heating to a temperature of 80 °C. The initiator, potassium persulfate (KPS), was then added to the solution to begin the polymerization reaction, which continued at 80 °C for one hour while being continuously stirred at 150 rpm. The obtained Poly(St-co-GMA-IDA) nanoparticles with an average size of about 250 nm were collected via centrifugation and washed multiple times with ethanol followed by drying and redispersing in DI water.

2.1.2. Electroless plating of silver nanoshells

To enable homogeneous and size-controlled deposition of silver nanoshells on the surface of the synthesized PS nanoparticles, we have developed a novel electroless plating protocol which is simple and scalable. The prepared Poly (St-co-GMA-IDA) nanoparticles or PS nanoparticles were added to silver nitrate (AgNO3) solution in DI water and the beaker was placed in a water bath whose temperature was controlled at 40 °C for 24 h. During this step, the positively charged silver ions are attracted to the negatively charged PS nanoparticles and act as seeds for further deposition of metallic silver. The modified PS nanoparticles are then filtered, washed and redispersed in DI water. Next, we freshly prepare the silver precursor solution which is Tollens' reagent (containing $[Ag(NH3)2]^+$ complex ions) and is obtained by reducing silver nitrate with ammonia. The PS nanoparticle solution is added to the Tollens reagent and heated at 50 °C for an hour after which glucose is added as the reducing agent and the reaction is allowed to continue for a further 20 min. The prepared PS/Ag nanoparticles are filtered, washed multiple times using a centrifuge and dried in an oven at 60 °C for an hour. Furthermore, the same reaction can be repeated multiple times to tune the size of the silver nanoshells which increase after each successful reduction reaction. The final step is to functionalize the surface of the silver nanoshells with amino groups using a heterobifunctional PEG ligand. In a typical process, 1.5 g of DI water, 3 g of ethanol (95 wt%) and 0.5 g of thiol-PEG-amine were mixed under magnetic stirring at room temperature for 3 h. Next, 3 g of the PS/Ag nanoparticle dispersed in 100 g of ethanol was added and the two solutions were mixed at 60 °C for an hour. The functionalized nanoparticles were washed and filtered followed by drying at 60 °C for 12 h, after which they can be used for antibody conjugation. We have used a pH meter (Suntex Instruments Co., TS-100) to analyze the change in solution conductivity before and after electroless plating. While the relative conductivity of the solution containing DI water and PS nanoparticles is about 3.5 μS/cm, it increases to around 280–300 μS/cm after modification with Ag nanoshells. The morphology of the PS nanoparticles before and after deposition is characterized using a Transmission electron microscope (TEM, Philips Tecnai G2 F20) with an operating voltage of 200 kV. Also, Powder X-ray diffraction (XRD, Bruker D2-PHASER) was performed to detect formation of multicrystalline phases associated with formation of the Ag nanoshells.

2.1.3. Antibody conjugation

Before antibody conjugation, the HSA antibodies are oxidized in a solution of 1 mM sodium metaperiodate and 0.1 M sodium acetate with the pH of 5.5. Next, the PS/Ag nanoparticles were added to the antibody solution and mixed under magnetic stirring at room temperature for 30 min. During this step, the hydroxyl groups in carbohydrate moieties of the antibodies are oxidized to aldehyde groups which can then react then with the amino groups present on the silver nanoshells of the PS/Ag nanoparticles via formation of a peptide bond. This allows the fragment crystallizable or Fc region of the antibody to be bound to the nanoparticle surface while the fragment antigen or Fab binding region is available during immunoassay. The PS/Ag/ab-HSA nanoprobes were washed multiple times in DI water to remove any unbound antibodies followed by dispersion in DI water and stored at 4 °C until further use. A spectrophotometer (Unico S1000 Visible Spectrophotometer) is used to perform optical density analysis and study the conjugation efficiency of ab-HSA to the PS/Ag nanoparticles. A 98% reduction in optical density of the supernatant before and after conjugation with ab-HSA as shown in Fig. 2d confirms that conjugation was successful.

2.2. Immunosensor fabrication

The carbon IMEs, fabricated on flexible PET sheets using a one-step screen-printing protocol, are shown in the photo in Fig. 2a. Screen-printing is carried out at a speed of 100 mm/s to print the IMEs where the width and spacing between interdigitated fingers is 100 μm and 150 μm, respectively. Both the sensing sites which include the test and control have an area of 6.485 mm^2 with 8 pairs of interdigitated fingers

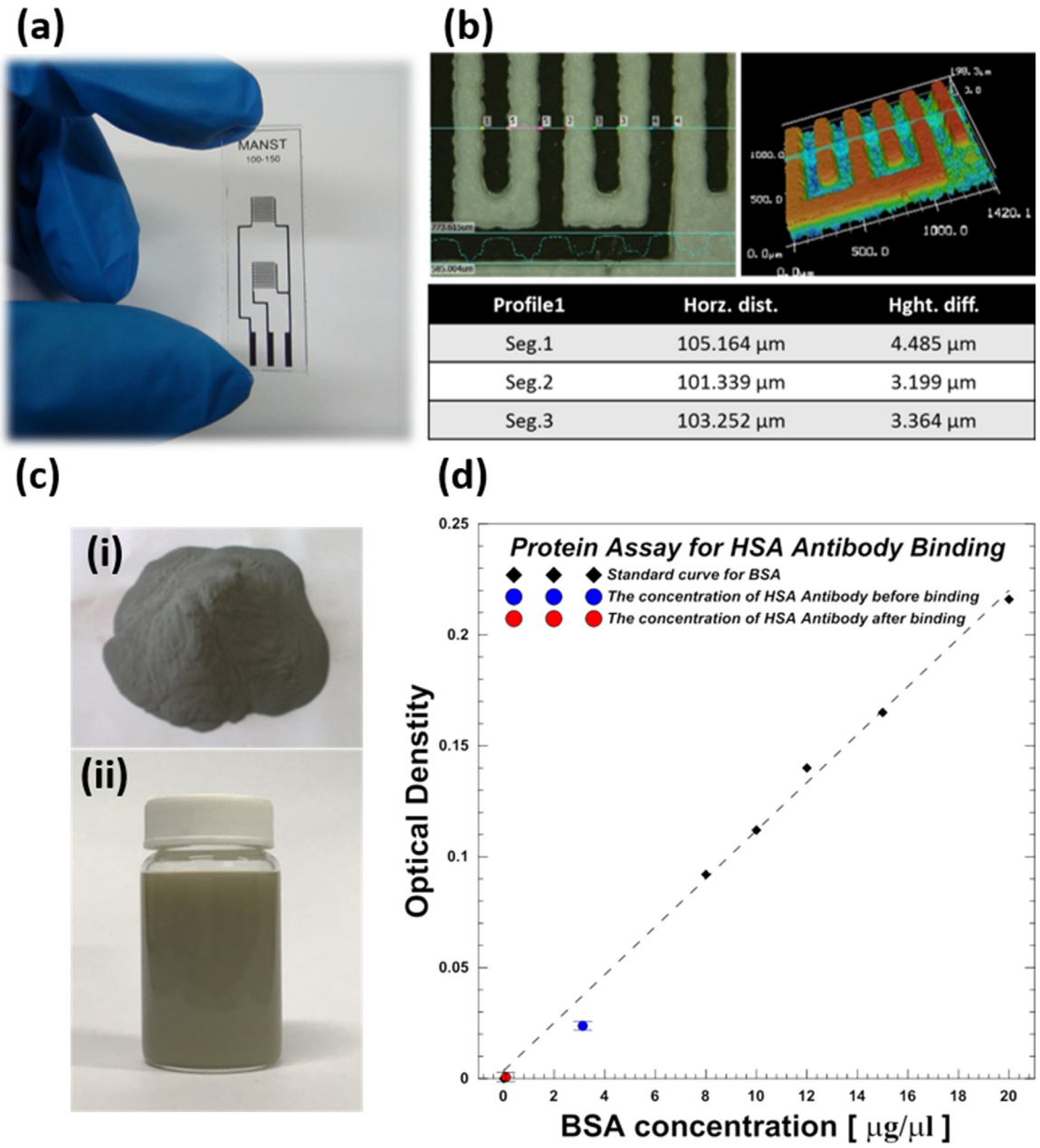

Fig. 2. (a) Photo of screen printed carbon IDEs on PET substrate. (b) Results of confocal microscopy to measure width and spacing of IDEs. (c) Photo of the PS/Ag nanoparticles as (i) powder and (ii) dispersed in DI water. (d) Optical density analysis confirms successful ab-HSA conjugation to the PS/Ag nanoparticles.

each. The ink used for printing is a commercially available conductive carbon paste (C-1011-6, Advanced Electronic Materials Inc. Taiwan). The printed electrodes are cured in a vacuum oven at 120 °C for 30 min to remove organic solvents present in the carbon paste and to improve its mechanical and electrical properties and provide better adhesion with the plastic substrate. An optical microscope (Olympus BX51M) is used to investigate the printed IMEs for any defects (e.g. development of cracks or short circuit connections) that may lead to erroneous readings. A confocal microscope (Keyence VK-X200K) is used to characterize IMEs finger width and spacing, and check the screen-printing conversion rate as schematically illustrated in Fig. 2b. We have also tested feasibility for electrochemical measurements of the screen-printed carbon IMEs by performing EIS and CV analysis in Phosphate Buffer Saline (PBS) solution and find good stability and repeatability after three scans as shown in Supplementary information (Fig. S1). Next, the electrodes are rinsed thoroughly with ultrapure water and allowed to dry the room temperature. The IMEs are now ready for further modification with gold (Au) nanocrystals which are electro-deposited in a 0.05 mM $HAuCl_4$ solution containing 0.5 M H_2SO_4 using linear sweep voltammetry (LSV) from −3V to 0 V at a scan rate of 0.05 V/s. The electrodeposition was carried out using an electro-chemical station (Metrohm Autolab, PGSTAT204) and a conventional three electrode setup with the carbon IMEs as the working electrode and a Pt wire and Ag/AgCl (saturated KCl) as the counter and reference electrodes, respectively. Next, the PS/Ag/ab-HSA nanoprobes are trapped on the IMEs using positive DEP force. 50 µl of nanoprobe suspension with a conductivity of 280–300 µS/cm was dropped on the sensing areas (PS/Ag/ab-HSA and PS/Ag on the test and control sites, respectively) using a micropipette and an AC signal of 10 V_{pp} at 100 kHz is applied for 60 min using a function generator (AFG3022, Tektronix) to trap the nanoprobes. The nanoprobe trapping step is followed by washing with DI water and the baseline impedance before immunosensing is recorded (Z_0), after which the immunosensor is ready for operation. The surface of the bare IMEs and after modification with

gold nanocrystals and nanoprobe trapping are characterized using a table top Scanning Electron Microscope (Phenom Pro Desktop SEM) operated at an accelerating voltage of 10 kV.

2.3. Immunosensor operation

Each step during electrode modification and immunosensor operation was confirmed by electrochemical impedance analysis in a 10 μM PBS solution using an LCR meter (Wayne Kerr Electronics, WK 6420) in a frequency range of 1–100 kHz at an applied AC voltage with amplitude of 10 mV. To check the feasibility of the immunosensor for quantitative detection of albumin, 50 μl of DI water spiked with different concentrations of HSA protein (30–300 mg/ml) was dropped onto the sensing areas to perform immunosensing for 30 min. This is followed by a washing step to remove any excess unbound proteins and the impedance after immunosensing is recorded (Z_1). The impedance response ($\triangle Z$) due to immunoreaction can be mathematically expressed as Z_1-Z_0. Each concentration is tested 10 times using different immunosensors to confirm repeatability. We have tried to eliminate differences in the initial resistance of each electrode by normalizing the impedance response ($\triangle Z/Z_0$) during immunosensing ($\triangle Z$) with the initial impedance observed at that particular electrode after nanoprobe trapping (Z_0). Furthermore, we have performed differential analysis (ratio of normalized impedance variation at test and control sites) to give the final value of the impedance response of the immunosensor which is calculated at an operating frequency of 10 kHz where we observe the maximum stable response. Differential analysis aids in eliminating non-specific binding effects and ensures that the impedance change after immunosensing is due to the formation of antibody/antigen complex and not because of the physical immobilization of proteins, thus reducing the chances of obtaining false positive results (Daniels and Pourmand, 2007).

3. Results and discussion

3.1. Core-shell PS/Ag functionalized nanoparticles

The morphology of the synthesized PS nanoparticles before and after electroless plating of silver nanoshells can be seen in the TEM images as shown in Fig. 3a-c. The PS nanoparticles obtained by dispersion polymerization are spherical with a smooth surface and have an average diameter of about 250 nm. The electroless plating protocol developed in this study results in uniform and evenly dispersed silver nanoshells on the surface of the PS nanoparticles. The obtained Ag nanoshells act as nucleation sites for further growth of metallic Ag using successive electroless plating cycles which involve the reduction reaction of Tollens reagent with glucose. It can be seen from the TEM images that the Ag nanoshells have an average diameter of about 5–10 nm after the first electroless plating cycle and grow to about 25 nm after two cycles. While this process could be repeated to eventually obtain complete coverage of the Ag shell on the PS core, it will result in lower effective surface areas as compared to dispersed Ag nanoshells. We have chosen to grow the Ag nanoshells to a size of about 25 nm as obtained after two electroless plating cycles, which can enable enhanced surface areas for increased antibody conjugation and consequently result in improved sensitivities. Powder XRD analysis was performed to confirm deposition of crystalline silver nanoshells on the PS core during electroless plating. The XRD spectrum, shown in Fig. 3d, shows a broad peak at 20.5° before silver deposition which is due to the amorphous structure of the PS nanoparticles. After electroless plating, the XRD spectra shows sharp distinct peaks whose 2θ values correspond to crystalline planes of cubic Ag. The obtained XRD results are in agreement with previously reports that have developed PS-Ag core shell particles (Zhang et al., 2012).

3.2. Electrode modification

The successful fabrication of an electrochemical immunosensor generally requires suitable modification of the electrode surface to enable improved sensitivity. The surface morphology of the bare screen printed IMEs and after electrodeposition of Au nanocrystals and dielectrophoretic trapping of PS/Ag nanoprobes can be seen in the SEM images in Fig. 4. After electrodeposition using LSV from −0.3 to 0 V, it was observed that surface of the carbon IMEs have a dense, uniform and conformal growth of gold nanocrystals which have an average size ranging from 50 to 100 nm. A major advantage of electrochemical deposition is the ability to control size and distribution of the Au nanocrystals by simply varying the potential range, scan rate or concentration of gold precursor. This process enables deposition in a short time at high growth rates and can be localized selectively on the surface of the working electrode without material wastage. These electrodeposited Au nanocrystals increase the conductivity of the bare electrode as shown by the lower observed impedance values in the bode plot in Fig. 5a. This improved charge transfer can result in stronger electric fields being generated across the IME fingers during DEP trapping. This effect, combined with the enhanced surface area and biocompatibility of the gold nanocrystals, can result in effective immobilization of the PS/Ag/ab-HSA nanoprobes. Consequently, DEP can successfully manipulate and trap the nanoprobes on modified electrode surface with good surface coverage when the applied voltage, frequency and immobilization time are optimized.

3.3. Feasibility of immunosensor for microalbuminuria detection

To confirm the feasibility of the proposed immunosensor for microalbuminuria detection, we have performed preliminary tests using PBS spiked with different concentrations of HSA. The impedance values observed at each step of electrode modification and after immunosensing are shown in the Bode plot in Fig. 5a. It can be seen that the impedance value at 10 kHz drops by about 8 kΩ after electrodeposition of Au nanocrystals on the bare carbon IMEs. These Au crystals significantly increase the surface area and act as nanoscale electrodes, which improves charge transfer between the interdigitated fingers, resulting in improved conductivity. After immobilization of the PS/Ag/ab-HSA nanoprobes using DEP, it was observed that the impedance increased to a value close to that of the bare electrode and further increased after immunosensing with 300 μg/ml of spiked HSA buffer solution. This is because both the PS core and the antibody-antigen complex are dielectric in nature and can be visualized as increasing the thickness of the dielectric layer in a capacitor (where the two conductive plates are the modified electrode and the buffer electrolyte). This effect results in reduced capacitance and an increase in overall impedance. Furthermore, the comparative impedance change observed at the test and control sites during immunosensing with 300 μg/ml of HSA spiked buffer solution is shown in Fig. 5b, c. The normalized impedance variation ($\triangle Z/Z_0$) when expressed as a percentage was 16.14% for the test site, which is significantly higher than the 3.24% observed for the control. While immunosensing due to antigen-antibody complex formation occurs at the test site, this is not the case at the control site, which only has trapped PS/Ag nanoparticles without any conjugated antibodies. However, there is still as small change at the control site due to non-specific binding of HSA on the modified electrode surface due to physical absorption. It is for this reason that we have included the capability of performing differential analysis $\left(Z = \frac{Z_{Test}}{Z_{Control}} = \frac{(Z_1 - Z_0)}{Z_0} Test / \frac{(Z_1 - Z_0)}{Z_0} Control\right)$, on the same chip which eliminates the effect of non-specific absorption and increases detection accuracy. The normalized immunosensor response after differential analysis was observed for different concentrations of HSA in the range of 30–300 μg/ml as shown in Fig. 5d. The normalized impedance variation after differential analysis shows a linear response to HSA

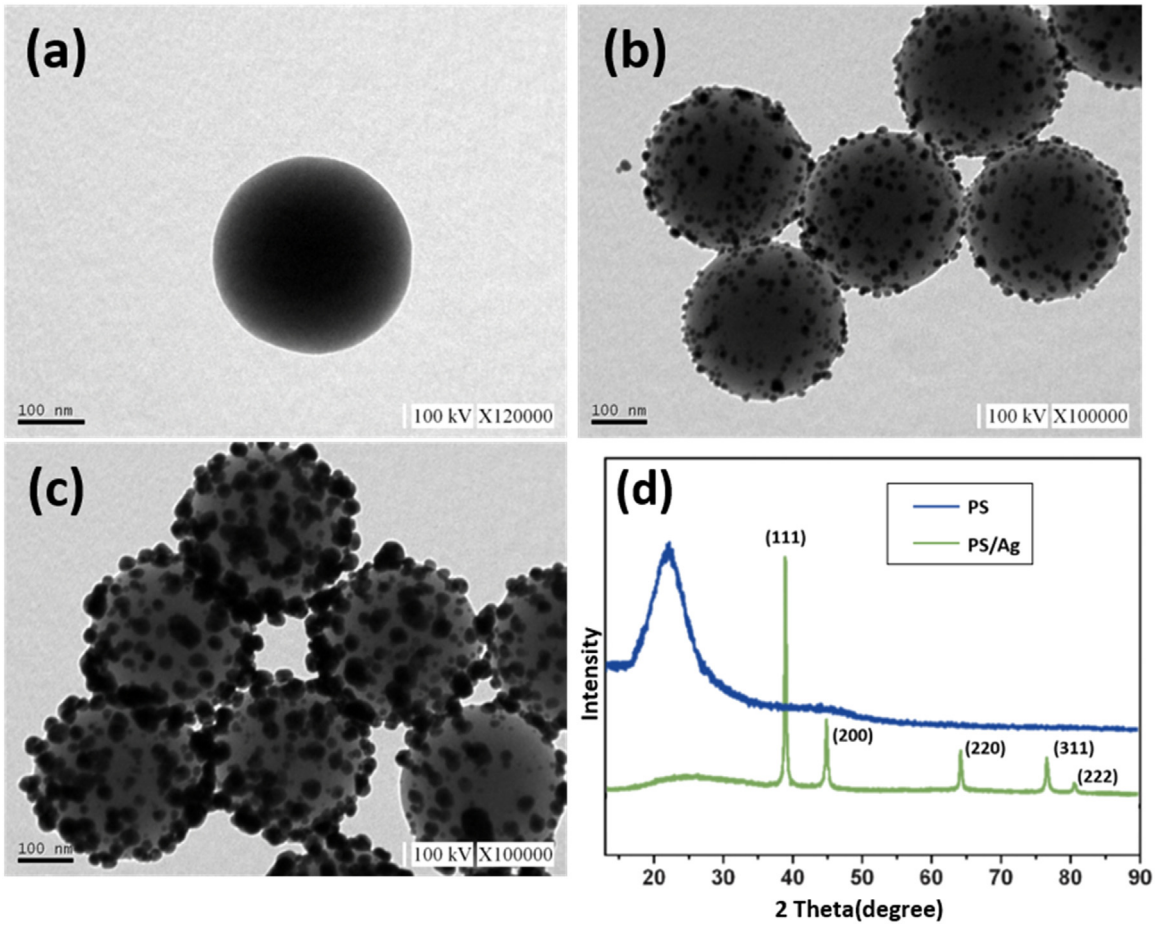

Fig. 3. TEM images of (a) PS nanoparticle (b) PS/Ag nanoparticles after one-step electroless plating and (c) after two-step electroless plating. (d) Powder XRD spectra of PS nanoparticles before and after Ag electroless plating.

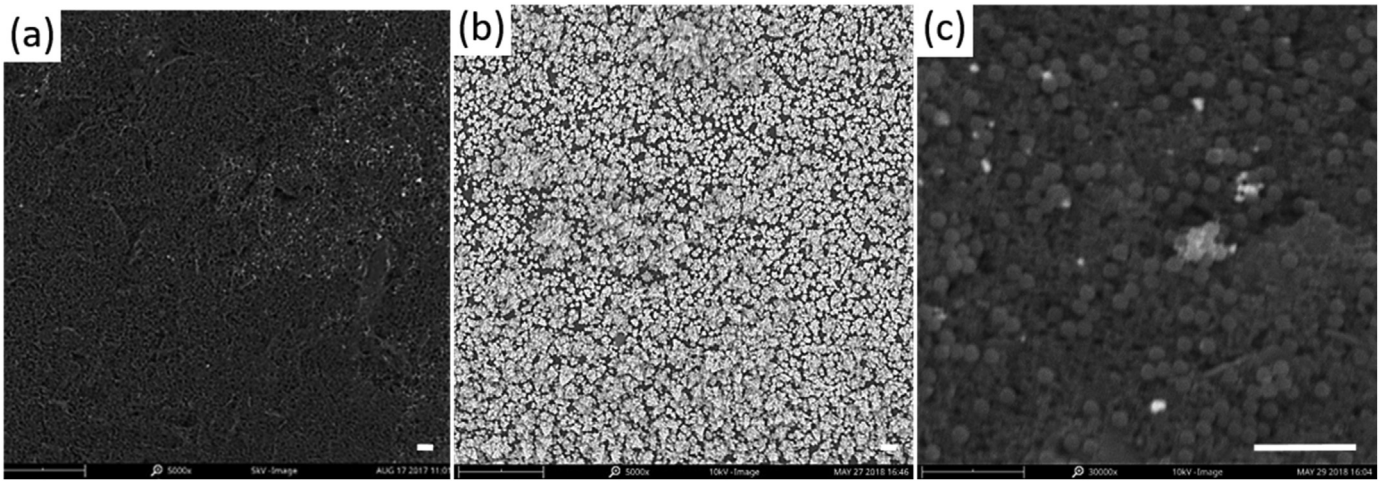

Fig. 4. SEM images of (a) bare screen printed carbon IMEs. (b) After electrodeposition of Au nanocrystals and (c) dielectrophoretic trapping of PS/Ag/ab-HSA nanoprobes (The scale bar corresponds to 2 μm).

concentration from 30 to 300 μg/ml with a coefficient of determination value of 0.98. Furthermore, the immunosensor response is stable and repeatable with low variability as shown by the short error bars obtained by testing each concentration using 10 different immunosensors. Consequently, the proposed immunosensor shows potential for quantitative screening of microalbuminuria. The next step will involve clinical testing using human urine samples and the results will be published in the near future.

3.4. Portable readout module for POC

To enable point of care testing using the proposed immunosensor, EIS analysis should be performed using a miniaturized and portable impedance analyzer as opposed to bulky and expensive LCR meters and potentiostats commonly used in laboratory settings. Therefore, we have developed a low cost prototype impedance readout module with dimensions of 8.5 cm × 4 cm × 5 cm and 3-D printed outer packaging as

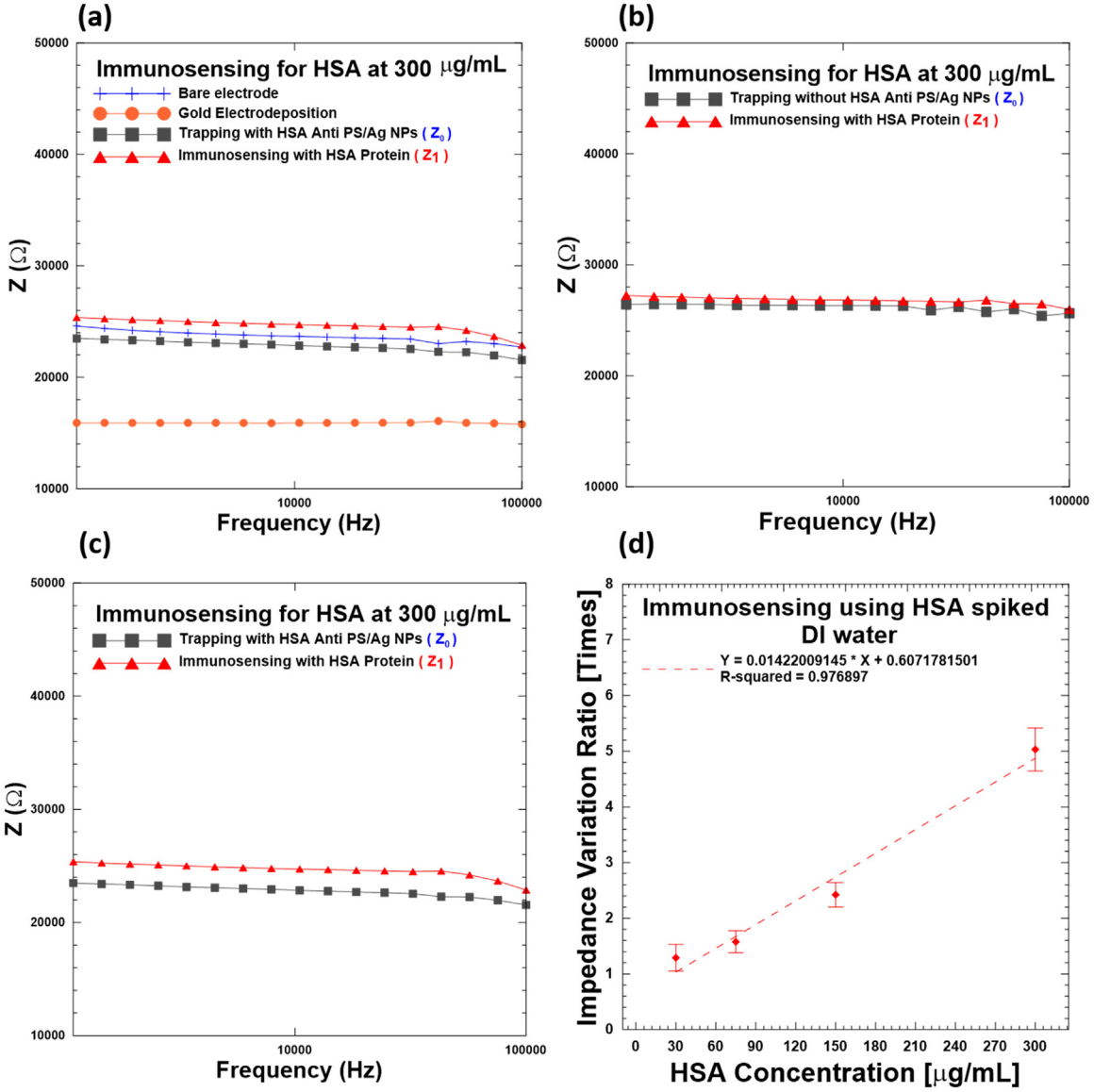

Fig. 5. (a) Impedance curves (bode plot) for each step during immunosensor modification and operation. Impedance response after immunosensing with 300 µg/ml HSA spiked buffer solution at the (b) Control and (c) Test site. (d) Normalized impedance variation after differential analysis for different HSA concentrations in the clinically relevant range required for detection of microalbuminuria.

shown in Fig. 6a, b. To enable size comparison, we have also provided a photo of the readout module placed beside a Taiwan currency 10 NTD coin as shown in Supplementary information (Fig. S2). When switched on, the device has a user friendly operation interface with an OLED display and is powered by a small rechargeable battery (3.7 V, 450 mAh). The device utilizes an Altera MAX10 system Field Programmable Gate Array (FPGA) module as shown in the block diagram in Fig. 6c with 12-bit ADC with sampling speed of 1Msps programmed using the hardware description language Verilog Syntax. The carrier signal of the direct digital synthesizer (DDS) is generated by the FPGA, and the back end is matched with the voltage control current source (VCCS) to generate a stable current. After testing, the impedance analysis is performed by the demodulation circuit and the information is integrated into the FPGA module through the I^2C communication protocol. Also, a pre-amplifier and calibration circuit is used to improve accuracy and stability by increased signal-noise ratio (SNR) during impedance analysis. Furthermore, the readout module uses Bluetooth Low Energy (BLE) to wirelessly transmit data to a mobile device like a smartphone or tablet which has an installed APP that we have developed to analyze the data and provide real time feedback. Uploading the data to a cloud database will allow the physician to track the patient's microalbuminuria levels over time and enable early detection and improved treatment and prognosis of kidney disease. Furthermore, we have compared the impedance measurements of the proposed readout module with a table-top LCR meter as shown in the table in Fig. 6d using standard resistors ranging from 200 to 1000 K, and find a maximum deviation of 3.05% which is observed for the 1000 K resistor. Consequently, we have developed a complete point of care immunosensing platform comprising of a disposable chip and a portable readout module.

4. Conclusions

In summary, we have developed a point of care immunosensing platform for the quantitative detection of microalbuminuria. The low cost and flexible plastic based immunosensor utilizes carbon IMEs fabricated via a simple one-step screen-printing protocol. The surface of the IMEs is modified with gold nanocrystals, which improves electrode conductivity, biocompatibility and charge transfer capability. Furthermore, we have synthesized novel PS/Ag/ab-HSA nanoprobes to

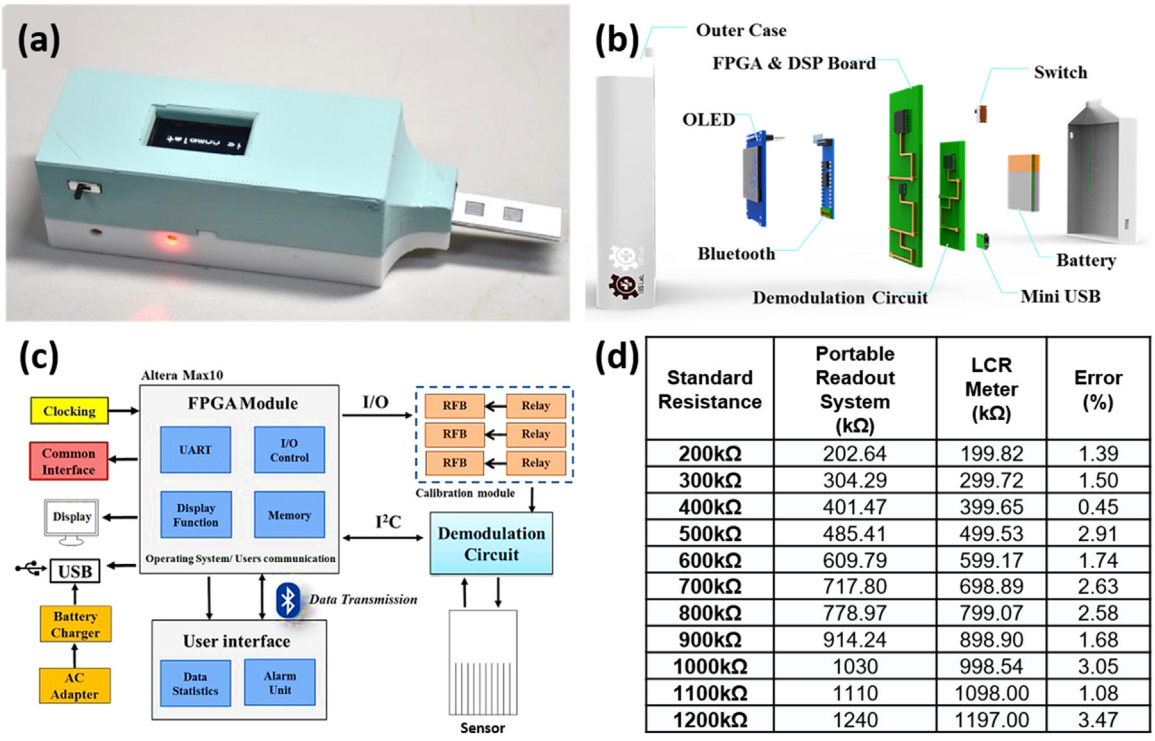

(d)

Standard Resistance	Portable Readout System (kΩ)	LCR Meter (kΩ)	Error (%)
200kΩ	202.64	199.82	1.39
300kΩ	304.29	299.72	1.50
400kΩ	401.47	399.65	0.45
500kΩ	485.41	499.53	2.91
600kΩ	609.79	599.17	1.74
700kΩ	717.80	698.89	2.63
800kΩ	778.97	799.07	2.58
900kΩ	914.24	898.90	1.68
1000kΩ	1030	998.54	3.05
1100kΩ	1110	1098.00	1.08
1200kΩ	1240	1197.00	3.47

Fig. 6. (a) Photograph, (b) Schematic of inner components and (c) Block diagram of the developed prototype impedance readout module. (d) Table showing comparison of the impedance measurements obtained using the readout module with a conventional laboratory LCR meter.

enable effective antibody immobilization using p-DEP. The proposed immunosensor can successfully detect microalbuminuria in the clinically relevant stage needed for early diagnosis of CKD with good repeatability. The ability to combine the disposable immunosensor chip with a portable impedance analyzer as developed in this study will enable effective point of care diagnosis, monitoring and prognosis of CKD.

Acknowledgements

The authors would like to thank the Ministry of Science and Technology, Taiwan, for financially supporting this research under Contract No. MOST 106–2632-E-218-001.

Appendix A. Supporting information

Supplementary data associated with this article can be found in the online version at doi:10.1016/j.bios.2018.11.035.

References

Abdorahim, Mojgan, Rabiee, Mohammad, Alhosseini, Sanaz Naghavi, Tahriri, Mohammadreza, Yazdanpanah, Sara, Alavi, S. Habib, Tayebi, Lobat, 2016. Nanomaterials-based electrochemical immunosensors for cardiac troponin recognition: an illustrated review. TrAC Trends Anal. Chem. 82, 337–347.

Athey, Dale, Ball, Mark, McNeil, Calum J., Armstrong, Ron D., 1995. A study of enzyme-catalyzed product deposition on planar gold electrodes using electrical impedance measurement. Electroanalysis 7 (3), 270–273.

Bardea, Amos, Patolsky, Fernando, Dagan, Arie, Willner, Itamar, 1999. Sensing and amplification of oligonucleotide-DNA interactions by means of impedance spectroscopy: a route to a Tay–Sachs sensor. Chem. Commun. 1, 21–22.

Chuang, C.H., Wu, T.F., Chen, C.H., Chang, K.C., Ju, J.W., Huang, Y.W., Van Nhan, V., 2015. Lab on a chip for multiplexed immunoassays to detect bladder cancer using multifunctional dielectrophoretic manipulations. Lab Chip 15 (14), 3056.

Chuang, Cheng-Hsin, Du, Yi-Chun, Wu, Ting-Feng, Chen, Cheng-Ho, Lee, Da-Huei, Chen, Shih-Min, Huang, Ting-Chi, Wu, Hsun-Pei, Shaikh, Muhammad Omar, 2016. Immunosensor for the ultrasensitive and quantitative detection of bladder cancer in point of care testing. Biosens. Bioelectron. 84, 126–132.

Chuang, C.H., Shaikh, M.O., 2017. "Label Free Impedance Biosensors for Point of Care Diagnostics". In Point-of-Care Diagnostics - New Progresses and Perspectives. IAPC-OBC Publishing, pp. 171–201.

Comper, Wayne D., Osicka, Tanya M., 2005. Detection of urinary albumin. Adv. Chronic Kidney Dis. 12 (2), 170–176.

da Silva, Everson T.S.G., Souto, Dênio E.P., Barragan, José T.C., Giarola, Juliana de F., de Moraes, Ana C.M., Kubota, Lauro T., 2017. Electrochemical biosensors in point-of--care devices: recent advances and future trends. ChemElectroChem 4 (4), 778–794.

Daniels, Jonathan S., Pourmand, Nader, 2007. Label-free impedance biosensors: opportunities and challenges. Electroanalysis 19 (12), 1239–1257.

Dincer, Can, Bruch, Richard, Kling, André, Dittrich, Petra S., Urban, Gerald A., 2017. Multiplexed point-of-care testing–xPOCT. Trends Biotechnol. 35 (8), 728–742.

Forman, John P., Fisher, Naomi D.L., Schopick, Emily L., Curhan, Gary C., 2008. Higher levels of albuminuria within the normal range predict incident hypertension. J. Am. Soc. Nephrol. 19 (10), 1983–1988.

Fu, Yusheng, Guo, Jinhong, 2018. Blood cholesterol monitoring with smartphone as miniaturized electrochemical analyzer for cardiovascular disease prevention. IEEE Trans. Biomed. Circuits Syst. 12 (4), 784–790.

Gauglitz, G.ünter, 2014. Point-of-care platforms. Annu. Rev. Anal. Chem. 7, 297–315.

Glassock, Richard J., 2010. Is the presence of microalbuminuria a relevant marker of kidney disease? Curr. Hypertens. Rep. 12 (5), 364–368.

Guo, Jinhong, 2017. Smartphone-powered electrochemical dongle for point-of-care monitoring of blood β-ketone. Anal. Chem. 89 (17), 8609–8613.

Guo, Jinhong, 2018. Smartphone-powered electrochemical biosensing dongle for emerging medical IoTs application. IEEE Trans. Ind. Inform. 14 (6), 2592–2597.

Guo, Jinhong, Ma, Xing, 2017. Simultaneous monitoring of glucose and uric acid on a single test strip with dual channels. Biosens. Bioelectron. 94, 415–419.

Guo, Jinhong, Huang, Xiwei, Ai, Ye, 2015. On-demand lensless single cell imaging activated by differential resistive pulse sensing. Anal. Chem. 87 (13), 6516–6519.

Guo, Jinhong, Huang, Xiwei, Ma, Xing, 2018. Clinical identification of diabetic ketosis/diabetic ketoacidosis acid by electrochemical dual channel test strip with medical smartphone. Sens. Actuators B: Chem. 275, 446–450.

Hezard, Teddy, Fajerwerg, Katia, Evrard, David, Collière, Vincent, Behra, Philippe, Gros, Pierre, 2012. Gold nanoparticles electrodeposited on glassy carbon using cyclic voltammetry: application to Hg (II) trace analysis. J. Electroanal. Chem. 664, 46–52.

Jefferson, J.A., Shankland, S.J., Pichler, R.H., 2008. Proteinuria in diabetic kidney disease: a mechanistic viewpoint. Kidney Int. 74 (1), 22–36.

Ju, HuangXian, 2011. Sensitive biosensing strategy based on functional nanomaterials. Sci. China Chem. 54 (8), 1202.

Kharitonov, Andrei B., Alfonta, Lital, Katz, Eugenii, Willner, Itamar, 2000. Probing of bioaffinity interactions at interfaces using impedance spectroscopy and chronopotentiometry. J. Electroanal. Chem. 487 (2), 133–141.

Lakowicz, Joseph R., Malicka, Joanna, Matveeva, Evgenia, Gryczynski, Ignacy, Gryczynski, Zygmunt, 2005. Plasmonic technology: novel approach to ultrasensitive immunoassays. Clin. Chem. 51 (10), 1914–1922.

Lim, Syazana Abdullah, Ahmed, Minhaz Uddin, 2016. Electrochemical immunosensors and their recent nanomaterial-based signal amplification strategies: a review. RSC Adv. 6 (30), 24995–25014.

Cardoso, M.M., Peca, I.N., Roque, A.C.A., 2012. Antibody-conjugated nanoparticles for therapeutic applications. Curr. Med. Chem. 19 (19), 3103–3127.
Magliano, Dianna J., Polkinghorne, Kevan R., Barr, Elizabeth L.M., Su, Qing, Chadban, Steven J., Zimmet, Paul Z., Shaw, Jonathan E., Atkins, Robert C., 2007. HPLC-detected albuminuria predicts mortality. J. Am. Soc. Nephrol. 18 (12), 3171–3176.
Omidfar, Kobra, Dehdast, Ahmad, Zarei, Hajar, Sourkohi, Behnoush Khorsand, Larijani, Bagher, 2011. Development of urinary albumin immunosensor based on colloidal AuNP and PVA. Biosens. Bioelectron. 26 (10), 4177–4183.
Pethig, Ronald, 2017. Where is dielectrophoresis (DEP) going? J. Electrochem. Soc. 164 (5), B3049–B3055.
Ricci, Francesco, Volpe, Giulia, Micheli, Laura, Palleschi, Giuseppe, 2007. A review on novel developments and applications of immunosensors in food analysis. Anal. Chim. 605 (2), 111–129.
Ronkainen, Niina J., Halsall, H. Brian, Heineman, William R., 2010. Electrochemical biosensors. Chem. Soc. Rev. 39 (5), 1747–1763.
Saber, Reza, Mutlu, Selma, Pişkin, Erhan, 2002. Glow-discharge treated piezoelectric quartz crystals as immunosensors for HSA detection. Biosens. Bioelectron. 17 (9), 727–734.
Taleat, Zahra, Khoshroo, Alireza, Mazloum-Ardakani, Mohammad, 2014. Screen-printed electrodes for biosensing: a review (2008–2013). Microchim. Acta 181 (9–10), 865–891.
Tsai, Jang-Zern, Chen, Ching-Jung, Settu, Kalpana, Lin, Yu-Feng, Chen, Chien-Lung, Liu, Jen-Tsai, 2016. Screen-printed carbon electrode-based electrochemical immunosensor for rapid detection of microalbuminuria. Biosens. Bioelectron. 77, 1175–1182.
Wen, Wei, Yan, Xu, Zhu, Chengzhou, Du, Dan, Lin, Yuehe, 2016. Recent advances in electrochemical immunosensors. Anal. Chem. 89 (1), 138–156.
Wu, Jie, Fu, Zhifeng, Yan, Feng, Ju, Huangxian, 2007. Biomedical and clinical applications of immunoassays and immunosensors for tumor markers. TrAC Trends Anal. Chem. 26 (7), 679–688.
Xu, Dandan, Huang, Xiwei, Guo, Jinhong, Ma, Xing, 2018. Automatic smartphone-based microfluidic biosensor system at the point of care. Biosens. Bioelectron.
Yang, Liju, Li, Yanbin, Erf, Gisela F., 2004. Interdigitated array microelectrode-based electrochemical impedance immunosensor for detection of Escherichia c oli O157: H7. Anal. Chem. 76 (4), 1107–1113.
Zhang, Chunjing, Zhu, Xianfang, Li, Haixia, Khan, Imran, Imran, Muhammad, Wang, Lianzhou, Bao, Jianjun, Cheng, Xuan, 2012. Controllable fabrication of PS/Ag core-shell-shaped nanostructures. Nanoscale Res. Lett. 7 (1), 580.